Open Access Series of Imaging Studies (OASIS): Longitudinal MRI Data in Nondemented and Demented Older Adults

Daniel S. Marcus[1], **Anthony F. Fotenos**[2], **John G. Csernansky**[3], **John C. Morris**[4], and **Randy L. Buckner**[5,6,7,8]

[1] Mallinckrodt Institute of Radiology, Washington University School of Medicine

[2] Washington University School of Medicine

[3] Department of Psychiatry, Northwestern University School of Medicine

[4] Department of Neurology, Washington University School of Medicine

[5] Department of Psychology, Harvard University, Cambridge, MA

[6] Department of Radiology, Harvard Medical School, Boston, MA

[7] Athinoula A. Martinos Center for Biomedical Imaging, Massachusetts General Hospital, Charlestown, MA

[8] Howard Hughes Medical Institute

Abstract

The Open Access Series of Imaging Studies (OASIS) is a series of neuroimaging data sets that is publicly available for study and analysis. The present MRI data set consists of a longitudinal collection of 150 subjects aged 60 to 96 all acquired on the same scanner using identical sequences. Each subject was scanned on two or more visits, separated by at least one year for a total of 373 imaging sessions. Subjects were characterized using the Clinical Dementia Rating (CDR) as either nondemented or with very mild to mild Alzheimer's disease (AD). 72 of the subjects were characterized as nondemented throughout the study. 64 of the included subjects were characterized as demented at the time of their initial visits and remained so for subsequent scans, including 51 individuals with CDR 0.5 similar level of impairment to individuals elsewhere considered to have 'mild cognitive impairment'. Another 14 subjects were characterized as nondemented at the time of their initial visit (CDR 0) and were subsequently characterized as demented at a later visit (CDR > 0). The subjects were all right-handed and include both men (n=62) and women (n=88). For each scanning session, 3 or 4 individual T1-weighted MRI scans were obtained. Multiple within-session acquisitions provide extremely high contrast-to-noise making the data amenable to a wide range of analytic approaches including automated computational analysis. Automated calculation of whole brain volume is presented to demonstrate use of the data for measuring differences associated with normal aging and AD.

Keywords

Address correspondence to: Daniel S. Marcus, Department of Radiology, Campus Box 8225, Washington University School of Medicine, 4525 Scott Ave., St. Louis, MO 63110, dmarcus@wustl.edu, Phone: 314-362-4562, Fax: 314-362-6110.

INTRODUCTION

The Open Access Series of Imaging Studies (OASIS) is a project aimed at making neuroimaging data sets of the brain freely available to the scientific community. By compiling and freely distributing neuroimaging data sets, we hope to facilitate future discoveries in basic and clinical neuroscience similar to other initiatives such as the Alzheimer's Disease Neuroimaging Initiative (ADNI). The initial OASIS set of cross-sectional MRI data included over 400 demented and nondemented individuals across the adult lifespan (Marcus et al., 2007a). Here we describe a longitudinal sample of MRI data from older adults, with and without Alzheimer's disease (AD). The preparation and release of the data set follows the rigor established with the initial release: careful quality control, detailed documentation, example postprocessed images, full anonymization, multiple access methods, ongoing support, and liberal data usage requirements (Marcus, et al., 2007a).

The data set includes longitudinal MRI data from 150 individuals age 60 to 96, including 64 individuals with very mild to moderate AD as diagnosed clinically and characterized using the Clinical Dementia Rating (CDR) scale (Morris, 1993; Morris et al., 2001) at their initial visit. Another 14 of the individuals were characterized as nondemented at the time of one or more scans and then clinically determined to have AD at the time of a subsequent scan. All data were acquired on the same scanner using identical procedures. Subjects were screened to eliminate individuals with psychiatric and neurological conditions that might contribute to dementia but, where possible, variation typical of advanced aging was included. Thus, many of the older adults had age-related increases in blood pressure and a small percentage treated diabetes. Sample characteristics were similar between the individuals with and without AD.

Longitudinal brain imaging has proven useful in studying normal and diseased aging. Whole brain volume decline as measured from longitudinally acquired MRI has been shown to evolve at a near 0.5% per year (in the range −0.37 to −0.88 across seven reports) (Chan et al., 2001; Wang et al., 2002; Liu et al., 2003; Resnick et al., 2003; Thompson et al., 2003; Jack et al., 2004; Fotenos et al., 2005) in nondemented older adults, somewhat greater than that observed in younger adults (Raz, 2005; Liu et al., 2003). The volumes of the whole brain and structures associated with memory have been shown to atrophy at a significantly greater rate in mild cognitive impairment and early AD (e.g., Jack et al., 1992, 1997; Fox et al., 1997; Kiliany et al., 2000, 2002; Dickerson et al., 2001; Fotenos et al., 2005). Longitudinal analysis of measures derived from advanced computational methods, including nonlinear deformations and shape analysis, have also revealed age- and disease-associated changes in the brain (e.g., Scahill et al., 2003; Thompson et al., 2003; Wang et al., 2003; Buckner et al., 2005). Longitudinal measures of brain structure are emerging as tools for tracking progression of disease and as adjunct outcome measures in clinical trials (e.g., Mueller et al., 2005; Chong et al., 2006; Borroni et al., 2007; Jack et al., 2007). The OASIS longitudinal data set is being made openly available to encourage continued investigation into aging and disease processes and to support development of improved methods for studying these processes.

METHODS

Subjects

Subjects aged 60–96 years were selected from a larger database of individuals who had participated in MRI studies at Washington University, based on the availability of at least two separate visits in which clinical and MRI data were obtained, at least three acquired T1-weighted images per imaging session, and right-hand dominance. Subjects were obtained from the longitudinal pool of the Washington University Alzheimer Disease Research Center (ADRC). The ADRC's normal and cognitively impaired subjects were recruited

primarily through media appeals and word of mouth, with 80% of subjects initiating contact with the center and the remainder being referred by physicians. All subjects participated in accordance with guidelines of the Washington University Human Studies Committee. Approval for public sharing of the anonymized data was also specifically obtained.

All subjects were screened for inclusion in this release. Each subject underwent the ADRC's full clinical assessment as described below. Subjects with a primary cause of dementia other than AD (e.g., vascular dementia, primary progressive aphasia), active neurologic or psychiatric illness (e.g. major depression), serious head injury, history of clinically meaningful stroke, and use of psychoactive drugs were excluded, as were subjects with gross anatomical abnormalities evident in their MRI images (e.g. large lesions, tumors). However, subjects with age-typical brain changes (e.g. mild atrophy, leukoaraiosis) were accepted. MRI acquisitions typically were obtained within one year before or after a subject's clinical assessment (mean = 111 days, range = 0 to 352 days). Twelve subjects with AD were scanned after a somewhat longer duration (mean = 653 days, range = 374 to 924 days) but were included because each had several previous clinical assessments with CDR scores greater than 0. Two subjects without dementia were scanned somewhat longer than one year prior to a clinical assessment (392 and 431 days) but were included because their subsequent clinical assessments continued to indicate no signs of dementia. Each subject was scanned on two or more separate occasions, with an average delay of 719 days (range = 183–1707 days) between visits. The final data set includes 150 subjects and 373 imaging sessions.

Portions of the clinical, demographic, and longitudinal image data obtained from subjects in this release have been used in previous publications (Buckner et al., 2004; Salat et al., 2004; Buckner et al., 2005; Head et al., 2005; Burns et al., 2005; Fotenos et al., 2005; Dickerson et al., 2007; Fotenos et al., 2008; Dickerson et al., 2008; He et al., 2008; Salat et al., 2008). Many of the subjects were part of the cross-sectional OASIS data set (Marcus et al., 2007) but have been assigned new random identifiers.

Clinical Assessment

Dementia status was established and staged using the CDR scale. The determination of AD or nondemented control status is based solely on clinical methods, without reference to psychometric performance, and any potential alternative causes of dementia (known neurological, medical, or psychiatric disorders) must not contribute to dementia. The diagnosis of AD is based on clinical information (derived primarily from a collateral source) that the subject has experienced gradual onset and progression of decline in memory and other cognitive and functional domains. Specifically, the CDR is a dementia staging instrument that rates subjects for impairment in each of 6 domains: memory, orientation, judgment and problem solving, function in community affairs, home and hobbies, and personal care. Based on the collateral source and subject interview, a global CDR score is derived from individual ratings in each domain. A global CDR of 0 indicates no dementia and CDR of 0.5, 1, 2 and 3 represent very mild, mild, moderate, and severe dementia, respectively. These methods allow for the clinical diagnosis of AD in individuals with a CDR of 0.5 or greater, based on standard criteria, that is confirmed by histopathological examination in 93% of the individuals (Berg et al., 1998), even for those in the earliest symptomatic stage (CDR 0.5) of AD who elsewhere may be considered to represent "mild cognitive impairment" (Storandt et al., 2006).

Image Acquisition

For each subject, 3 to 4 individual T1-weighted magnetization prepared rapid gradient echo (MP-RAGE) images were acquired on a 1.5-Tesla Vision scanner (Siemens, Erlangen,

Germany) in a single imaging session. Head movement was minimized by cushioning and a thermoplastic face mask. Headphones were provided for communication. A vitamin E capsule was placed over the left forehead to provide a reference marker of anatomic side. Positioning was low in the head coil (toward the feet) to optimize imaging of the cerebral cortex. MP-RAGE parameters were empirically optimized for gray-white contrast (Table 1). The scanner and sequences were maintained across the duration of the study so the present data are not influenced by hardware upgrades or other instrument differences.

Postprocessing

For each subject, the individual scan files were converted from Siemens proprietary IMA format into 16-bit NiFTI1 format using a custom conversion program. Header fields with identifying information (patient ID, experiment date) were left blank. The images were then corrected for inter-scan head movement and spatially warped into the atlas space of Talairach and Tournoux (1988) using a rigid transformation that differs in process from the original piecewise scaling. The resulting transformation nonetheless places the brains in the same coordinate system and bounding box as the original atlas. The template atlas used here consisted of a combined young-and-old target previously generated from a representative sample of young ($n = 12$) and nondemented old ($n = 12$) adults. The use of a combined template has been shown to minimize the potential bias of an atlas normalization procedure to over-expand atrophied brains (Buckner et al., 2004). Given the age range of the present sample, an old-only atlas target could have been employed. We chose to retain the young-and-old target to be comparable to our earlier report (Marcus et al., 2007a).

For registration, a 12-parameter affine transformation was computed to minimize the variance between the first MP-RAGE image and the atlas target. The remaining MP-RAGE images were registered to the first (in-plane stretch allowed) and resampled via transform composition into a 1-mm isotropic image in atlas space. The result was a single, high-contrast, averaged MP-RAGE image in atlas space. Subsequent steps included skull removal by application of a loose-fitting atlas mask and correction for intensity inhomogeneity due to nonuniformity in the magnetic field. Intensity variation was corrected across contiguous regions, based on a quadratic inhomogeneity model fitted to data from a phantom.

Estimated Total Intracranial Volume (eTIV) and Normalized Whole-brain Volume (nWBV)

The procedures used for measuring intracranial and whole-brain volumes have been described previously (Buckner et al., 2004; Fotenos et al., 2005) and are identical to our earlier OASIS data release (Marcus et al., 2007a). eTIV was computed by scaling the manually-measured intracranial volume of the atlas by the determinant of the affine transform connecting each individual's brain to the atlas. This method is minimally influenced and proportional to manually measured total intracranial volume.

nWBV was computed using the FAST program in the FSL software suite (www.fmrib.ox.ac.uk/fsl). The image was first segmented to classify brain tissue as cerebral spinal fluid (CSF), gray, or white matter. The segmentation procedure iteratively assigned voxels to tissue classes based on maximum likelihood estimates of a hidden Markov random field model. The model used spatial proximity to constrain the probability with which voxels of a given intensity are assigned to each tissue class. Finally, nWBV was computed as the proportion of all voxels within the brain mask classified as tissue (either gray or white matter). The unit of normalized volume is percent, which represents the percentage of the total white and gray matter voxels within the estimated total intracranial volume (Fotenos et al., 2005). To calculate atrophy rates, we estimated the slope of the line connecting nWBV measurements within each individual, divided by baseline nWBV, expressed as percent change per year. For example, in a participant with two scans, atrophy rate was computed as

nWBV at scan 2 minus nWBV at scan 1, divided by the interval between measurements, divided by nWBV at scan 1, times 100. Analysis of covariance was again used to test for differences in atrophy rate based on age, sex, and dementia status.

Quality Control

All images in the data set were carefully screened for artifacts, acquisition problems, and processing errors. During the screening process, each image was viewed on a per-slice basis along the axis of acquisition. Typical flaws visible in the images included electronic noise resulting in bright lines through multiple slices, motion artifacts appearing as hazy bands across the image, poor head positioning resulting in wraparound artifacts, distortions from dental work, and limited image contrast. Images with severe flaws were excluded from the data set. A number of borderline images remain in the distribution, providing tool builders and testers with a realistic range of acquisition quality. In cases where individual scans were deemed unusable, the single scan was removed from the data set but the remainder of the subject's scans was included. Overall, 25 imaging sessions were excluded from the final release due to poor image quality.

RESULTS

Overview of the data set

The current data set consists of 150 subjects (88 female) aged 60–96 (Table 2). At the time of their initial visit 86 had a CDR score of 0, indicating no dementia, and 64 had a CDR score greater than zero (52 CDR 0.5, 13 CDR 1, 0 CDR 2), indicating a diagnosis of very mild to moderate AD. Of the subjects who were initially determined to be nondemented, 14 were later determined to be demented (CDR > 0) at the time of a subsequent imaging visit. Additional demographics and clinical characteristics of the subjects are shown in Table 3.

Anatomic characteristics

Whole brain volumes for each of the subjects in the dataset are plotted by age at each visit in Figure 1. Marked decreases in nWBV are apparent with age, and nWBV is significantly impacted by dementia status (Figure 2). Differences in nWBV between non-demented (CDR 0), very mild dementia (CDR 0.5), and mild dementia (CDR 1) are all significant (p<0.01). Whole brain atrophy rates are shown in Figure 3 (top). The atrophy rate in nondemented individuals was −0.49% (SD = 0.56) per year. The atrophy rate in individuals with DAT was −0.87% (SD = 0.99) per year, a significant increase compared with nondemented individuals (p<0.01). For the 14 individuals who declined from an initial CDR 0 to a CDR 0.5 at the time of their last scan, the atrophy rate fell between nondemented individuals and those who entered with AD (−0.69% per year, SD = 0.62).

Obtaining and using the data

OASIS data can be obtained at http://www.oasis-brains.org. Requests for DVD distributions of the data can be submitted at the website. For convenience, we also provide the data using the open-source Extensible Neuroimaging Archive Toolkit (XNAT) (Marcus et al., 2007b). It provides tools to search, visualize, and download the data. Prior to downloading and requesting data, users are asked to abide by the OASIS Data Usage Agreement.

OASIS data are distributed in GNU zip archive files which can be uncompressed using freely available software. All images are distributed in NIFTI1 format (http://nifti.nimh.nih.gov), which can be visualized and processed using many common commercial and open source image viewing applications, including Neurolens, ImageJ, Slicer, and MRIcro. For each imaging session, the following image files are included in the distribution: 3–4 individual scan images; an image in which the individual scans have been

aligned and co-registered, an image that has been gain field-corrected and registered to the Talairach and Tournoux atlas (T88); a masked T88 image in which the intensity of all non-brain voxels has been set to zero; and a segmented T88 image in which each voxel has been labeled as grey matter, white matter, or CSF. Demographic, clinical, and derived imaging measures (Table 4) are available in XML and spreadsheet formats. Additional details of the directory structure, file naming scheme, and image characteristics can be found at http://www.oasis-brains.org/longitudinal_facts.html.

The present data set includes longitudinally acquired T1-weighted MRI data from 150 individuals aged 60 to 96, including 64 individuals initially determined to have AD and 14 who were diagnosed with AD at a return visit. Repeated within-visit acquisitions are included for each subject allowing extremely high contrast properties after image averaging. The data have been anonymized, carefully screened for image quality, and post-processed to generate common anatomic measures. The data are available under a liberal usage policy that allows free access and unrestricted usage to all interested parties.

The image files included in this OASIS set differ from the previous OASIS set in two substantive ways meant to improve overall usability. First, the files are in the NiFTI 1 image format, which is now widely supported and preferred for its more explicit specification of voxel ordering. Second, the images have not been altered to remove facial features. This ensures that fiducial markers placed on the left temple are always present in raw scan images. It also removes hard edges that may cause difficulty in some segmentation algorithms.

The specific anatomical measure of nWBV included here illustrates a common approach to analyzing anatomical characteristics of the brain in MRI images, particularly in relation to aging. Unsurprisingly, our findings are in agreement with those described in previous studies using portions of these data (e.g. Fotenos et al., 2005). In particular, nWBV was shown to decline significantly with increasing age and by AD status as previously reported by Fotenos et al. (2005) and others (Jack et al., 1992, 1997; Fox et al., 1997; Kiliany et al., 2000, [2002]; Dickerson et al., 2001). Similarly, the rate of nWBV decline was significantly greater for the AD group than for the nondemented group.

These findings are representative of the types of analyses that have been reported in the literature and are not intended to be comprehensive or the final word on how to approach these data. Such issues as the interplay between imaging markers, AD, and other diseases (e.g. hypertension, diabetes) remain open avenues for further investigation. Similarly, alternative image processing and statistical methods may yield additional findings. We hope that the description and open release of these data will encourage ongoing exploration of the data, leading to improvements in the diagnosis and treatment of Alzheimer's disease.

Supplementary Material

Refer to Web version on PubMed Central for supplementary material.

Acknowledgments

References

Beckett LA, deToledo-Morrell L. MRI-derived entorhinal and hippocampal atrophy in incipient and very mild Alzheimer's disease. Neurobiology of Aging 2001;22:747–754. [PubMed: 11705634]

Berg L, McKeel DW, Miller JP, et al. Clinicopathologic studies in cognitively healthy aging and Alzheimer disease relation of histologic markers to dementia severity, age, sex, and apolipoprotein E genotype. Archives of Neurology 1998;55:326–335. [PubMed: 9520006]

Borroni B, Premi E, Di Luca M, Padovani A. Combined biomarkers for early Alzheimer disease diagnosis. Current Medicinal Chemistry 2007;14:1171–1180. [PubMed: 17504137]

Buckner RL, Snyder AZ, Shannon BJ, LaRossa G, Sachs R, Fotenos AF, Sheline YI, Klunk WE, Mathis CA, Morris JC, Mintun MA. Molecular, structural, and functional characterization of Alzheimer's disease: evidence for a relationship between default activity, amyloid, and memory. Journal of Neuroscience 2005;25:7709–7717. [PubMed: 16120771]

Buckner RL, Head D, Parker J, Fotenos AF, Marcus DS, Morris JC, Snyder AZ. A unified approach for morphometric and functional data analysis in young, old, and demented adults using automated atlas-based head size normalization: reliability and validation against manual measurement of total intracranial volume. Neuroimage 2004;23:724–738. [PubMed: 15488422]

Burns JM, Church JA, Johnson DK, Xiong C, Marcus D, Fotenos AF, Snyder AZ, Morris JC, Buckner RL. White matter lesions are prevalent but differentially related with cognition in aging and early Alzheimer disease. Archives of Neurology 2005;62:1870–1876. [PubMed: 16344345]

Chan D, Fox NC, Jenkins R, Scahill RI, Crum WR, Rossor MN. Rates of global and regional cerebral atrophy in AD and frontotemporal dementia. Neurology 2001;57:1759–1763.

Chong MS, Lim WS, Sahadevan S. Biomarkers in preclinical Alzheimer's disease. Current Opinion in Investigational Drugs 2006;7:600–607. [PubMed: 16869111]

Dickerson BC, Goncharova I, Sullivan MP, Forchetti C, Wilson RS, Bennett DA, Storandt M, Grant EA, Miller JP, Morris JC. Longitudinal course and neuropathologic outcomes in original vs revised MCI and in pre-MCI. Neurology 2006;67:467–473. [PubMed: 16894109]

Dickerson BC, Feczko E, Augustinack JC, Pacheco J, Morris JC, Fischl B, Buckner RL. Differential effects of aging and Alzheimer's disease on medial temporal lobe cortical thickness and surface area. Neurobiology of Aging (epub). 2007

Dickerson BC, Bakkour A, Salat DH, Feczko E, Pacheco J, Greve DN, Grodstein F, Wright CI, Blacker D, Rosas HD, Sperling RA, Atri A, Growdon JH, Hyman BT, Morris JC, Buckner RL. The cortical signature of Alzheimer's disease: regionally-specific cortical thinning relates to symptom severity in very mild to mild AD dementia and is detectable in asymptomatic amyloid-positive individuals. Cerebral Cortex. 2008

Du AT, Schuff N, Chao LL, Kornak J, Jagust WJ, Kramer JH, et al. Age-effects on atrophy rates of entorhinal cortex and hippocampus. Neurobiol Aging 2006;27:733–740. [PubMed: 15961190]

Fotenos AF, Snyder AZ, Girton LE, Morris JC, Buckner RL. Normative estimates of cross-sectional and longitudinal brain volume decline in aging and AD. Neurology 2005;64:1032–1039. [PubMed: 15781822]

Fotenos AF, Mintun MA, Snyder AZ, Morris MD, Buckner RL. Brain volume decline in aging: Evidence for a relation between socioeconomic status, preclinical Alzheimer's disease, and reserve. Arch Neurology 2008;65:113–120.

Fox NC, Freeborough PA. Brain atrophy progression measured from registered serial MRI: validation and application to Alzheimer's disease. Journal of Magnetic Resonance Imaging 1997;7:1069–1075. [PubMed: 9400851]

He Y, Chen Z, Evans A. Structural insights into aberrant topological patterns of large-scale cortical networks in Alzheimer's disease. J Neurosci 2008;28:4756–66. [PubMed: 18448652]

Head D, Snyder AZ, Girton LE, Morris JC, Buckner RL. Frontal-hippocampal double dissociation between normal aging and Alzheimer's disease. Cerebral Cortex 2005;15:732–739. [PubMed: 15371293]

Hollingshead, A. Two Factor Index of Social Position. New Haven, CT: Yale University Press; 1957.

Jack CR Jr, Petersen PC, O'Brien, Tangalos EG. MR-based hippocampal volumetry in the diagnosis of Alzheimer's disease. Neurology 1992;62:183–188. [PubMed: 1734300]

Jack CR Jr, Petersen RC, Xu YC, et al. Medial temporal atrophy on MRI in normal aging and very mild Alzheimer's disease. Neurology 1997;49:786–794. [PubMed: 9305341]

Jack CR Jr, Shiung MM, Gunter JL, et al. Comparison of different MRI brain atrophy rate measures with clinical disease progression in AD. Neurology 2004;62:591–600. [PubMed: 14981176]

Jack CR Jr, Petersen RC, Grundman M, Jin S, Gamst A, Ward CP, Sencakova D, Doody RS, Thal LJ. Members of the Alzheimer's Disease Cooperative Study (ADCS). Longitudinal MRI findings from the vitamin E and donepezil treatment study for MCI. Neurobiology of Aging. 2007 in press.

Killiany RJ, Gomez-Isla T, Moss M, Kikinis R, Sandor T, Jolesz F, Tanzi R, Jones K, Hyman BT, Albert MS. Use of structural magnetic resonance imaging to predict who will get Alzheimer's disease. Annals of Neurology 2000;47:430–439. [PubMed: 10762153]

Killiany RJ, Hyman BT, Gomez-Isla T, Moss MB, Kikinis R, Jolesz F, Tanzi R, Jones K, Albert MS. MRI measures of entorhinal cortex vs hippocampus in preclinical AD. Neurology 2002;58:1188–1196. [PubMed: 11971085]

Liu R, Lemieux L, Bell GS, et al. A longitudinal study of brain morphometrics using quantitative magnetic resonance imaging and difference image analysis. Neuroimage 2003;20:22–33. [PubMed: 14527567]

Marcus DS, Wang TH, Parker J, Csernansky JG, Morris JC, Buckner RL. Open Access Series of Imaging Studies (OASIS): cross-sectional MRI data in young, middle aged, nondemented, and demented older adults. Journal of Cognitive Neuroscience 2007a;19:1498–1507. [PubMed: 17714011]

Marcus DS, Olsen TR, Ramaratnam M, Buckner RL. The Extensible Neuroimaging Archive Toolkit: an informatics platform for managing, exploring, and sharing neuroimaging data. Neuroinformatics 2007b;5:11–3.4. [PubMed: 17426351]

Morris JC. The Clinical Dementia Rating (CDR): current version and scoring rules. Neurology 1993;43:2412–2414. [PubMed: 8232972]

Morris JC, Storandt M, Miller JP, et al. Mild cognitive impairment represents early-stage Alzheimer disease. Archives of Neurology 2001;58:397–405. [PubMed: 11255443]

Mueller SG, Weiner MW, Thal LJ, Petersen RC, Jack CR, Jagust W, Trojanowski JQ, Toga AW, Beckett L. Ways toward an early diagnosis in Alzheimer's disease: The Alzheimer's Disease. Neuroimaging Initiative (ADNI). Alzheimers Dement 2005;1:55–60. [PubMed: 17476317]

Raz N, Lindenberger U, Rodrigue KM, Kennedy KM, Head D, Williamson A, Dahle C, Gerstorf D, Acker JD. Regional Brain Changes in Aging Healthy Adults: General Trends, Individual Differences and Modifiers. Cerebral Cortex 2005;15:1676–1689. [PubMed: 15703252]

Resnick SM, Pham DL, Kraut MA, Zonderman AB, Davatzikos C. Longitudinal magnetic resonance imaging studies of older adults: a shrinking brain. Journal of Neuroscience 2003;23:3295–3301. [PubMed: 12716936]

Salat DH, Buckner RL, Snyder AZ, Greve DN, Desikan RSR, Busa E, Morris JC, Dale AM, Fischl B. Thinning of the cerebral cortex in aging. Cerebral Cortex 2004;14:721–730. [PubMed: 15054051]

Salat DH, Greve DN, Pacheco JL, Quinn BT, Helmer KG, Buckner RL, Fischl B. Regional white matter volume differences in nondemented aging and Alzheimer's disease. Neuroimage. 2008

Scahill RI, Schott JM, Stevens JM, Rossor MN, Fox NC. Mapping the evolution of regional atrophy in Alzheimer's disease: unbiased analysis of fluid-registered serial MRI. Proceedings of the National Academy of Sciences 2002;99:4703–4707.

Thompson PM, Hayashi KM, de Zubicaray G, et al. Dynamics of gray matter loss in Alzheimer's disease. Journal of Neuroscience 2003;23:994–1005. [PubMed: 12574429]

Thompson PM, Hayashi KM, de Zubicaray G, Janke AL, Rose SE, Semple J, Herman D, Hong MS, Dittmer SS, Doddrell DM, Toga AW. Dynamics of gray matter loss in Alzheimer's disease. Journal of Neuroscience 2003;23:994–1005. [PubMed: 12574429]

Wang DM, Doddrell DM. MR image-based measurement of rates of change in volumes of brain structures. Part 1: method and validation. Magnetic Resonance Imaging 2002;20:27–40. [PubMed: 11973027]

Wang L, Swank JS, Glick IE, Gado MH, Miller MI, Morris JC, Csernansky JG. Changes in hippocampal volume and shape across time distinguish dementia of then Alzheimer type from healthy aging. Neuroimage 2003;20:667–682. [PubMed: 14568443]
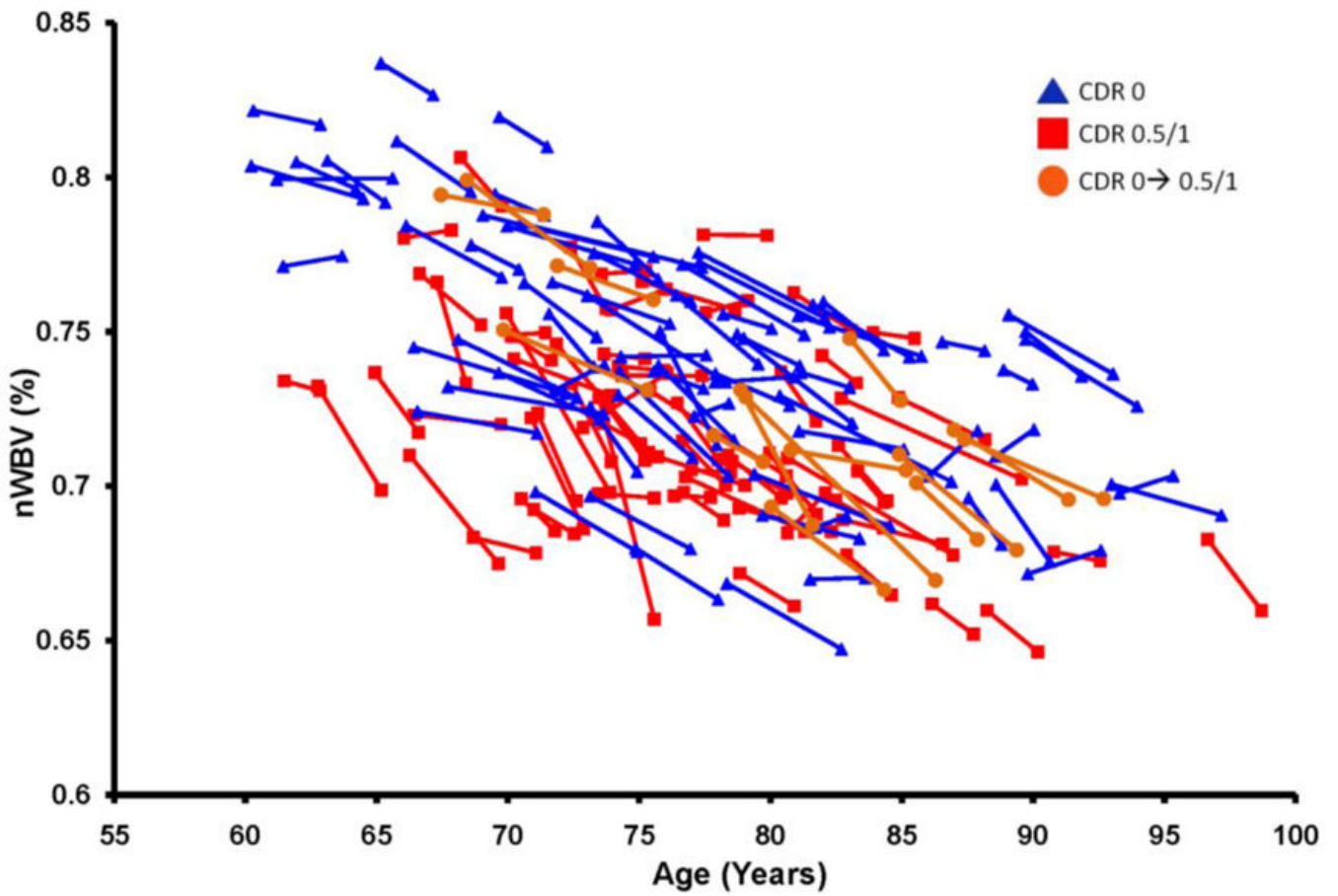
Figure 1.
Longitudinal plot of nWBV; lines connect nWBV at baseline and follow-up scans (or the best fit, for participants with multiple follow-ups), such that the slope of each line as a proportion of baseline nWBV represents an individual' atrophy rate.
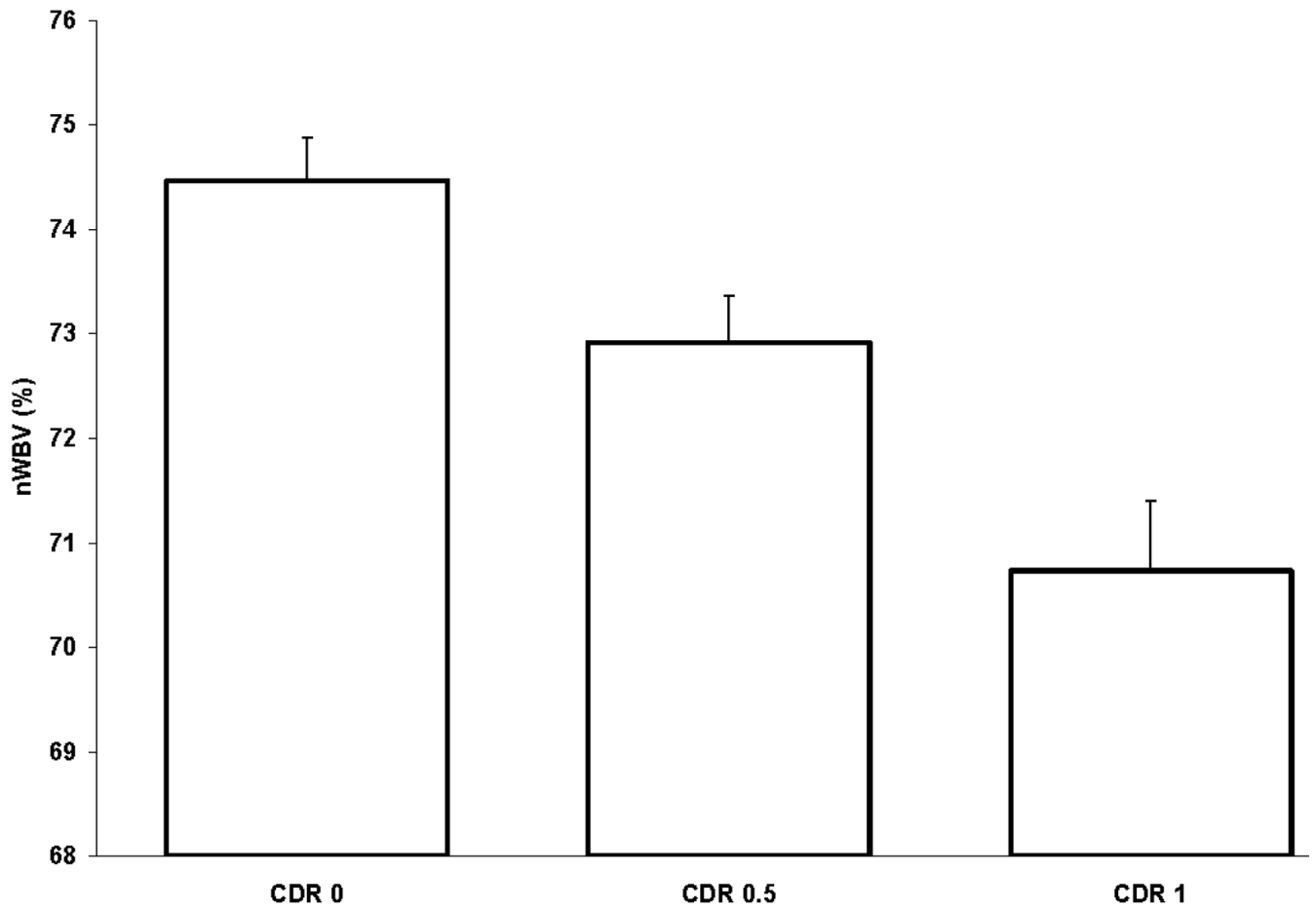
Figure 2.
Mean cross-sectional normalized whole-brain volume (nWBV) for all individuals separated
by Clinical Dementia Rating (CDR) (0, 0.5, and 1) at the individuals' initial visit. All
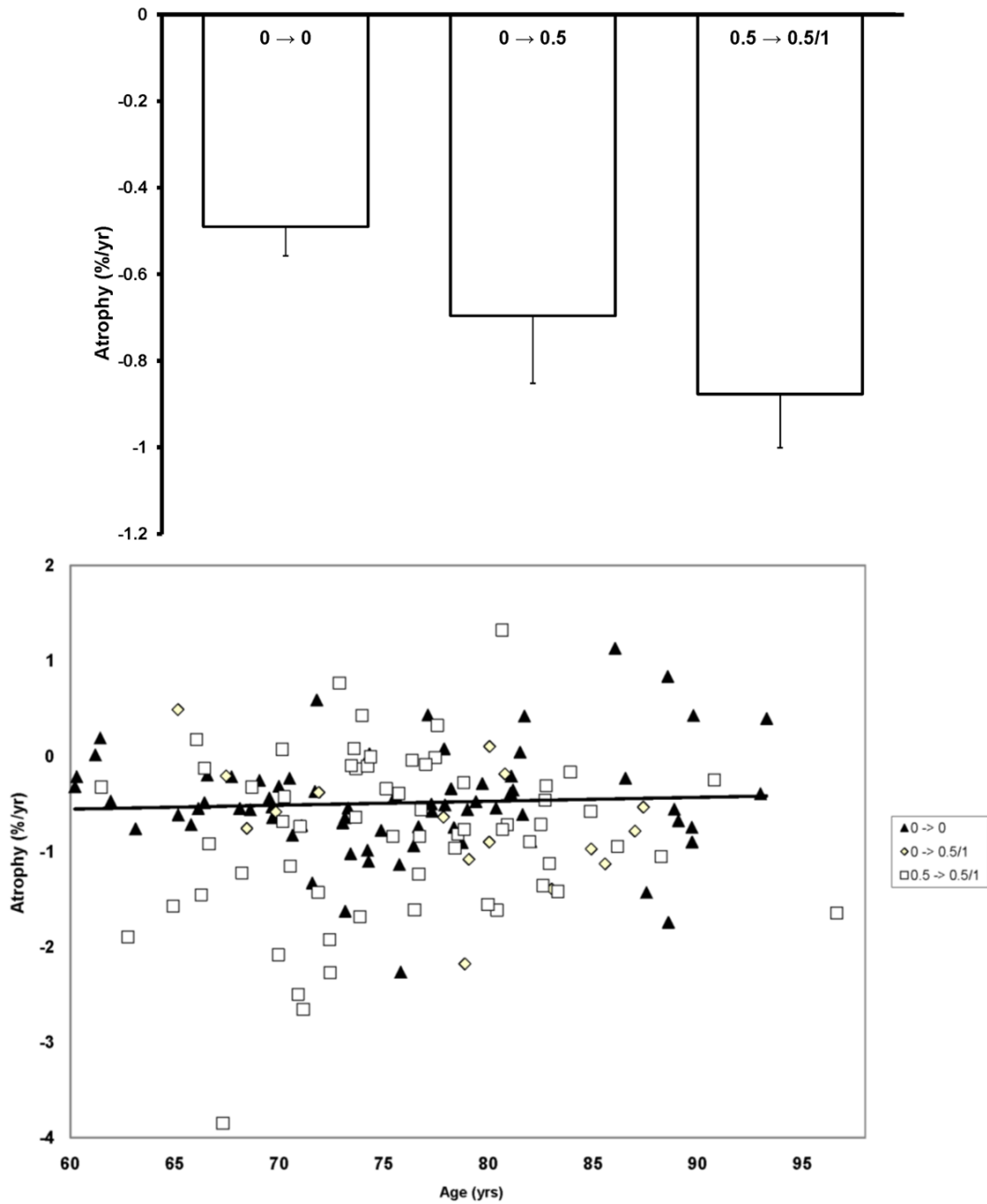differences are significant.

Figure 3.
(top) Longitudinal atrophy rates, expressed in nWBV loss per year relative to baseline, are separated by CDR status at first and last session. Atrophy rate was significantly greater for the group entering the experiment with very mild dementia (CDR $0.5 \rightarrow 0.5/1$) than the group entering without dementia that remained stable (CDR $0 \rightarrow 0$) while the rate for the group that manifested the earliest signs of AD during the experiment (CDR $0 \rightarrow 0.5$) fell between those with no dementia and those who entered with dementia. (bottom) Individual atrophy rates plotted by age and CDR score. The trendline is plotted for CDR $0 \rightarrow 0$.

Table 1

MR image acquisition details

Sequence	MP-RAGE
TR (ms)	9.7
TE (ms)	4.0
Flip angle	10°
TI (ms)	20
TD (ms)	200
Orientation	Sagittal
Thickness, gap (mm)	1.25, 0
Slice number	128
Resolution	256×256 (1×1 mm)

Table 2

Age and diagnosis characteristics of subjects at the time of their initial visit.

Age Group	N	Nondemented					Demented				
		n	mean	male	female	convert	n	Mean	male	female	CDR 0.5/1
60s	34	23	65.71	6	17	3	11	65.67	8	3	8/3
70s	71	35	74.91	11	24	4	36	73.97	20	16	29/7
80s	41	26	84.30	9	17	7	15	82.33	7	8	13/2
90s	4	2	92.50	0	2	0	2	93.00	1	1	1/1
Total	**150**	**86**	**75.82**	**26**	**59**	**14**	**64**	**74.95**	**36**	**29**	**52/13**

The **convert** column indicates individuals who were determined to have AD on a subsequent visit. CDR = Clinical Dementia Rating, with 0, 0.5, and 1 corresponding to nondemented, very mild, and AD. CDR 0.5 individuals may be considered to represent those elsewhere labeled as 'mild cognitive impairment' (MCI).

Table 3

Sample characteristics of subjects.

	CDR 0	**CDR 0.5**	**CDR 1**
Number	86	51	13
Female/male	60/26	21/30	7/6
Age, y	75.8 ± 8.2 (60–93)	74.8 ± 6.3 (62–90)	75.7 ± 8.7 (61–96)
Education, y	15.2 ± 2.7 (8–23)	13.6 ± 2.8 (6–20)	14.0 ± 3.2 (8–20)
MMSE	29.1 ± 0.8 (27–30)	26 ± 3.1 (17–30)	23.0 ± 3.3 (19–30)
Prescriptions, n	2.9 ± 2.1 (0–9)	3.2 ± 2.4 (0–11)	2.5 ± 2.4 (0–7)
Systolic BP, mmHg	135.5 ± 20.3 (98–192)	143.5 ± 19.4 (118–188)	143.4 ± 24.9 (90–188)
Diastolic BP, mmHg	72.8 ± 10.2 (50–100)	77.1 ± 10.1 (58–98)	76.9 ± 9.2 (60–88)
Reported HBP, %	54.6	46.0	53.3
Diabetes, %	9.3	14.0	13.3

The sample consisted of 150 individuals (72 nondemented, 64 with AD, and 14 who converted over the course of the study). Clinical measures in the above table were obtained at the clinical assessment closest in date to the initial imaging session, except in 39 cases where these values were not available until a later visit. Mean values given ± SD. Values in parentheses represent the range. Compared to the nondemented adults, the older adults with dementia had lower scores on the MMSE ($p < 0.001$) and slightly fewer years of education ($p < 0.001$).

CDR = Clinical Dementia Rating, with 0, 0.5, and 1 corresponding to nondemented, very mild, and mild AD; MMSE = Mini-Mental State Examination where scores range from 30 (best) to 0 (worst); HBP = high blood pressure.

Table 4

Measures included in the data set.

Age	Age at time of image acquisition (years).
Gender	Gender (M or F)
Education	Years of education
SES	Socioeconomic status as assessed by the Hollingshead Index of Social Position and classified into categories from 1 (highest status) to 5 (lowest status) (Hollingshead, 1957)
MMSE	Mini-Mental State Examination score (range is from 0 [worst] to 30 [best]) (Folstein, Folstein, & McHugh, 1975)
CDR	Clinical Dementia Rating. (0 = no dementia, 0.5 = very mild AD, 1 = mild AD, 2. = moderate AD) (Morris, 1993)
ASF	Atlas scaling factor (unitless). Computed scaling factor that transforms native-space brain and skull to the atlas target (i.e. the determinant of the transform matrix) (Buckner et al., 2004)
eTIV	Estimated total intracranial volume (cm^3) (Buckner et al., 2004)
nWBV	Normalized whole brain volume, expressed as a percent of all voxels in the atlas-masked image that are labeled as gray or white matter by the automated tissue segmentation process (Fotenos et al., 2005)